High Resolution Spectroscopy of the Hydrogen Atom: Determination of the 1S Lamb Shift

S. Bourzeix, B. de Beauvoir, F. Nez, M. D. Plimmer, F. de Tomasi, L. Julien, and F. Biraben
Laboratoire Kastler Brossel, Ecole Normale Supérieure et Université Pierre et Marie Curie, Laboratoire associé au CNRS URA18, 4 place Jussieu, Tour 12 E01, 75252 Paris Cedex 05, France

D. N. Stacey
Clarendon Laboratory, Parks Road, Oxford OX1 3PU, United Kingdom
(Received 1 August 1995)

We have measured the 1S Lamb shift by comparing the frequencies of the $1S_{1/2}$-$3S_{1/2}$ and $2S_{1/2}$-$6S_{1/2}$ or $2S_{1/2}$-$6D_{5/2}$ two-photon transitions. Our result is 8172.798 (46) MHz. It is the most precise yet reported and is consistent with the larger existing proton radius measurement of $r_p = 0.862(12)$ fm.

PACS numbers: 32.30.Jc, 06.20.Jr, 12.20.Fv, 42.65.Ky

For some fifty years, quantum electrodynamics (QED) calculations have steadily improved for bound atomic systems and now give the energy levels of the hydrogen atom to an impressive accuracy, of order 10^{-11} [1]. The hydrogen level energy is conventionally expressed as the sum of three terms: The energy given by the Dirac equation for a particle with the reduced mass, the first relativistic correction due to the recoil of the proton, and the Lamb shift. The first two terms are exactly known, apart from the uncertainties in the physical constants involved (the Rydberg constant R_∞, the fine structure constant, and the electron-to-proton mass ratio). The Lamb shift contains all the other corrections, i.e., the QED corrections, the other relativistic corrections due to the proton recoil, and the effect of the proton charge distribution. Precise measurements of the Lamb shift are required to test QED calculations or, if we suppose these calculations exact, to determine the proton charge radius. This last point is important, because there are two inconsistent measurements of the proton radius, $r_p = 0.805(11)$ and 0.862(12) fm [2,3]. Further, precise values of the Lamb shifts are essential to deduce R_∞ from recent optical measurements of hydrogen frequencies [4,5].

The so-called 2S Lamb shift (in fact the difference of the $2S_{1/2}$ and $2P_{1/2}$ Lamb shifts) is deduced from radio-frequency measurements of the $2S_{1/2}$-$2P_{1/2}$ splitting, the first by Lamb and Retherford [6]. The precision is now limited by the 2P natural width (100 MHz) [7,8]. The 1S Lamb shift is 8 times larger but is much more difficult to measure, since the 1S level is isolated. Up to now, all measurements of the 1S Lamb shift have been obtained from the study of the 1S-2S two-photon transition by subtracting the 1S-2S Dirac and recoil energies from the 1S-2S experimental result [9–11]. This subtraction is made by comparing the 1S-2S frequency with 4 times the 2S-4S, 2S-4P, or 2S-4D frequencies. Here the main limitations to further accuracy are the natural widths of the $n = 4$ levels (700 kHz, 12.9, and 4.4 MHz for the S, P, and D levels, respectively) and the low probabilities of the 2S-4S/D two-photon transitions. Another possibility is to use higher 2S-nS/D transitions. In this paper we present a measurement of the 1S Lamb shift deduced from the comparison of the 1S-3S and 2S-6S/D frequencies, which are also in the ratio 4:1. The 2S-6S and 2S-6D transitions are narrower (300 kHz and 1.3 MHz, respectively) and stronger than the 2S-4S and 2S-4D. To exploit this advantage, uncertainty due to light shifts, greater for the two-photon transitions due to stray electric fields is also larger (by a factor of 17), but the effect in this case is negligible. The 1S-3S transition is much weaker than the 1S-2S (by a factor of 140 with a cw laser of 50 kHz bandwidth), and much broader, but this line is not the limiting factor. With this method, we have measured the Lamb shift with an uncertainty of 5.6 parts in 10^6.

Figure 1 shows the general scheme of our experiment. A home-made titanium-sapphire laser at 820 nm is used to excite the two-photon transitions, either the 2S-6S/D or, after two frequency doubling steps, the 1S-3S. The laser frequency is actively stabilized by locking to a cavity using an FM sideband method, and the jitter is reduced to the level of 5 kHz. The long term stability is guaranteed

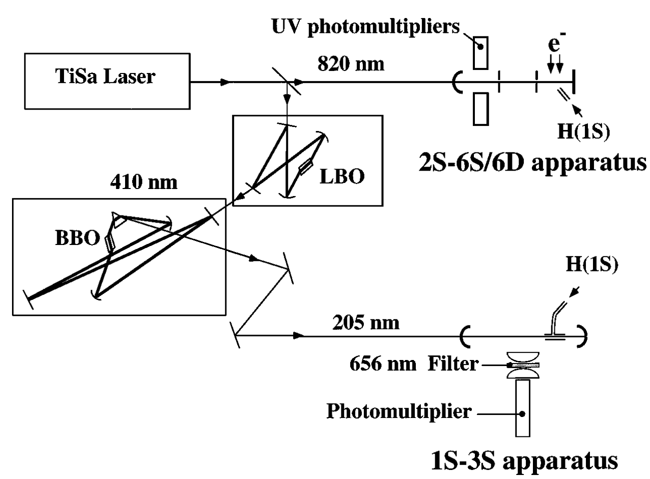

FIG. 1. Experimental setup for the frequency comparison between the 1S-3S and 2S-6S/D transitions.

 0031-9007/96/76(3)/384(4)$06.00

by the use of a second Fabry-Pérot reference cavity (FPR), which is frequently locked to an iodine stabilized He-Ne laser at 633 nm: the laser frequency is reproducible to 2 kHz day to day and to about 10 kHz over a year.

The 205 nm UV radiation is produced by two successive frequency doubling stages with two enhancement cavities. The first step, using a LBO crystal, has been described elsewhere [12] and provides up to 500 mW at 410 nm for a pump power of 2.3 W at 820 nm. The UV light is produced in a BBO crystal, 14 mm long, cut at the Brewster angle and placed inside a four-mirror astigmatically compensated ring cavity (BBO cavity). In the crystal the waist is 27 μm, and the UV light is extracted from the cavity using an intracavity prism. This second doubling step is far more challenging for several reasons. (i) The nonlinear coefficient d_{eff} is only 0.25 pm/V (for comparison, in the case of the $1S$-$2S$ transition, the generation of the 243 nm radiation involves a nonlinear coefficient d_{eff} of 1.39 pm/V). (ii) Rapid damage of the BBO crystal occurs during UV production, with a time constant of about 1 min, due probably to photochemical reactions on the faces of the crystal. However, we found that with the crystal inside a clean chamber filled with oxygen, the lifetime of a point on the crystal increases to about 15 min. (iii) After a few minutes, a counterpropagating wave at 410 nm begins to appear in the ring cavity, probably due to a photorefractive effect in the bulk of the BBO crystal. To reduce these effects, we have worked in a quasicontinuous regime where the UV intensity consists of 3 μs pulses at a frequency of 30 kHz. This is done by modulating the length of the BBO cavity so as to be resonant only some of the time. Under these conditions, despite the low duty cycle, the mean square power (which is involved in the probability of the two-photon transition) is higher than one can get by continuous locking. We obtain 1 mW peak power at 205 nm for several hours with the same point on the crystal. This modulation produces a frequency shift, the UV frequency being upshifted (downshifted) by about 125 kHz when the length of the BBO cavity decreases (increases).

To reduce transit time broadening the $1S$-$3S$ Doppler free two-photon signal is observed with an effusive atomic beam collinear with the UV beams. The atoms are produced from molecular hydrogen by a radio-frequency discharge linked to the vacuum apparatus by a 9 cm length of Teflon tube. After correction of the astigmatism, the UV beam emerging from the BBO crystal is mode matched to a third, linear, buildup cavity (two spherical mirrors with 25 cm radius of curvature) surrounding the atomic beam. Inside the cavity the beam waist is 50 μm and the UV power about 10 mW. The length of this cavity is locked to the UV frequency so that successive UV pulses have the same intensity inside the cavity. In these conditions, the frequency shifts of two successive UV pulses cancel and the residual frequency shift is estimated to be smaller than 3 kHz. The two-photon transition is detected by monitoring, through an interference filter, the $3S$-$2P$ fluorescence. The total background is about 160 counts s^{-1} and the $1S$-$3S$ signal 10 counts s^{-1} [Fig. 2(a)]. Each point in the figure corresponds to an acquisition time of about 1100 s. The experimental linewidth (1.7 MHz in terms of atomic frequency) is made up of the 1 MHz $3S$ natural width, the laser jitter (8 times 5 kHz), the transit time broadening (about 200 kHz), the second-order Doppler effect (about 100 kHz), and broadening due to the modulation of the UV light (about 500 kHz).

The $2S$-$6S/D$ apparatus is similar to the one used to measure the Rydberg constant [13,14]. The transitions are induced in a metastable atomic beam collinear with two counterpropagating laser beams. The atomic beam is produced by molecular dissociation followed by electron impact [15], and it is placed inside an enhancement cavity where the optical power can be as much as 130 W in each direction with a beam waist of 670 μm. To measure the metastable yield, an electric field quenches the $2S$ metastable atoms at the end of the atomic beam, and we detect the Lyman-α fluorescence. When the laser frequency is resonant with the $2S$-$6S/D$ transition, optical quenching of the metastable atoms occurs and we detect the corresponding decrease of the metastable beam intensity. In the recording shown in Fig. 2(b) the linewidth is about 2.5 MHz (in terms of atomic frequency). The $6D$ natural width is 1.3 MHz; the broadening is mainly due to the inhomogeneous light shift experienced by the atoms through the Gaussian profile of the laser beams. The light shift is also a major source of shift; we allow for it by recording the atomic signal for different laser intensities. For each recording, we fit a theoretical profile which takes into account the light shift and the saturation of the transition [13], enabling us to deduce the unperturbed position of the line.

We have made two series of measurements to compare, by means of the FPR cavity, the $1S$-$3S$ transition with the $2S_{1/2}$-$6D_{5/2}$ and $2S_{1/2}$-$6S_{1/2}$ transitions. For the first, we collected successively the data for the $2S$-$6D$ transition (1 day), the $1S$-$3S$ (3 days), and the $2S$-$6D$ once

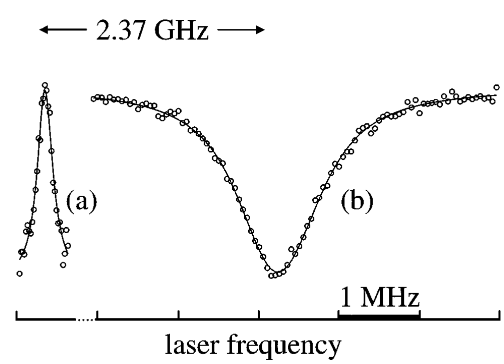

FIG. 2. Hydrogen two-photon spectra: (a) $1S(F = 1)$-$3S(F = 1)$ transition, (b) $2S_{1/2}(F = 1)$-$6D_{5/2}$ transition.

again (2 days). We used the same procedure to study the $2S_{1/2}$-$6S_{1/2}$ transition, but, due to its low intensity, the acquisition times were longer (4, 3, and 4 days, respectively). The results (i.e., the laser frequency splitting between the $1S$-$3S$ and $2S$-$6S/D$ lines), given in the first line of Table I, are multiplied by 8 to deduce the $1S$ Lamb shift (a factor of 4 for the two frequency doublings and 2 for the two-photon excitation). The quoted uncertainties (35 and 71 kHz for each measurement, one standard deviation) are mainly due to the uncertainties in the position of the $1S$-$3S$ line (19 and 24 kHz for each measurement) and of the $2S$-$6D$ or $2S$-$6S$ lines (28 and 66 kHz). We estimate the uncertainty due to a possible drift of the laser frequency during the experiment to be 8×1 kHz. The free spectral range of our FPR cavity is very precisely known by interferometry, the reference frequencies being the iodine stabilized He-Ne laser (633 nm) and the $2S$-$6D$ and $2S$-$8D$ hydrogen transitions (820 and 778 nm). The second-order Doppler effect is evaluated from the velocity distribution of the metastable atoms [4], and we estimate the shift of the $2S$-$6S/D$ line to be 37.8(1.9) kHz. Taking into account the electronic excitation of the metastable atoms, we can deduce the velocity distribution of the $1S$ atoms at the exit of the radio-frequency discharge. As the two discharges of the two atomic beams are of identical design, we can estimate the velocity distribution of the $1S$ atomic beam and calculate a second-order Doppler shift of 124(10) kHz for the $1S$-$3S$ transition. The Zeeman effect of the $2S$-$6S/D$ transitions is made negligible by means of a magnetic shield. For the $1S$-$3S$ transition, a residual magnetic field of 270 mG induces a quadratic Zeeman shift of about 1 kHz. A graphite coating of the two-vacuum apparatus reduces stray electric fields, and the residual Stark shifts are estimated to be smaller than 100 Hz. Finally, the light shift of the $1S$-$3S$ transition is also negligible (660 Hz at the center of the Gaussian beam).

The deduction of the $1S$ Lamb shift is detailed in Table I. After corrections for the hyperfine structure and the Dirac and relativistic recoil energies, we obtain the linear combination of Lamb shifts $L_{1S} - L_{3S} + 4L_{6S/D} - 4L_{2S}$. We have used the experimental value of the $2S_{1/2}$-$2P_{1/2}$ (the weighted mean value from Refs. [7,8]) and the theoretical values of the $2P$, $3S$, and $6S/D$ Lamb shifts. We have taken into account all the recent calculations of the high order terms following Ref. [1], particularly the two-loop QED corrections [16] and the more recent calculation of the $m/M\ (Z\alpha)^6$ term [17]. Using $r_p = 0.862$ fm, we obtain $L_{2P} = -12.8356(20)$ MHz, $L_{3S} = 311.403(2)$ MHz, $L_{6S} = 39.0859(3)$ MHz, and $L_{6D} = 0.1660(2)$ MHz. The two values obtained for the $1S$ Lamb shift are in good agreement and give a weighted mean value of 8172.798(46) MHz. This value, the most precise to date, is in good agreement with previous measurements (Table II) and with the theoretical value using the large proton radius [8172.802(40) MHz]. With the small proton radius, the disagreement is 2.3 standard deviations. If we assume the validity of the QED calculations, we can deduce a value of the proton radius $r_p = 0.861(20)$ fm.

In all these experiments, a large part of the uncertainty arises from the experimental value of the $2S$ Lamb shift. In the future, a way to avoid this limitation will be to use the $1/n^3$ scaling law of the Lamb shift. The quantity $L_{1S} - 8L_{2S}$ can be calculated very precisely, because all the terms varying exactly as $1/n^3$ (and particularly the effect of the size of the proton) disappear. For instance, from our experiment, we deduce the quantity $L_{1S} - 4L_{2S}$ [3992.768(34) MHz]. Using this result alone, together with the theoretical value of $L_{1S} - 8L_{2S}$ [$-187.236(11)$ MHz [19]], we obtain values of the $1S$ and $2S$ Lamb shifts [$L_{1S} = 8172.772(69)$ MHz and $L_{2S\text{-}2P} = 1057.837(9)$ MHz]. For the $2S$ Lamb shift, this result agrees very well with the microwave measurements [1057.845(9) MHz [7] and 1057.839(12) MHz [8]] but disagrees slightly with the indirect measurement of Pal'chikov, Sokolov, and Yakovlev [1057.8514(19) MHz [20]]. To exploit the potential of this approach, one needs very precise optical frequency measurements. For this reason, we intend to measure the optical frequency of the $1S$-$3S$ transition with respect to the cesium clock. The second-order Doppler effect, which is the major source of shift, will be canceled by the use of an appropriate

TABLE I. Determination of the $1S$ Lamb shift (frequency unit MHz).

	$2S_{1/2}$-$6D_{5/2}$	$2S_{1/2}$-$6S_{1/2}$
Laser frequency splitting	2370.1249(43)	2120.1714(88)
Laser frequency splitting $\times 8$	18 960.999(35)	16 961.371(19)
$2S$-$6S/D$ second-order Doppler effect	$4 \times 0.0378(19)$	$4 \times 0.0378(19)$
$1S$-$3S$ second-order Doppler effect	$-0.124(10)$	$-0.124(10)$
$1S$-$3S$ Zeeman effect	0.001	0.001
Hyperfine corrections	-164.6552	-170.9683
Dirac and recoil contributions	$-15\,114.3572$	$-12\,952.6568$
$L_{1S} - L_{3S} + 4(L_{6S/D} - L_{2S})$	3682.015(37)	3837.774(72)
$4(L_{2S} - L_{2P})$ (experiment)	4231.372(29)	4231.372(29)
$L_{3S} + 4L_{2P} - 4L_{6S/D}$ (theory)	259.3965(83)	103.7169(84)
$1S$ Lamb shift	8172.783(48)	8172.863(78)

TABLE II. Some recent measurements of the 1S Lamb shift and comparison with theory (MHz).

Transitions	1S Lamb shift
1S-2S and 2S-4S/D [a]	8172.820(110)
1S-2S and 2S-8S/D [b]	8172.815(70)
1S-2S and 2S-4S [c]	8172.860(60)
1S-2S and 2S-4P [d]	8172.827(51)
This work	8172.798(46)
Theory ($r_p = 0.862$ fm)	8172.802(40)
Theory ($r_p = 0.805$ fm)	8172.653(40)

[a]Reference [18].
[b]Reference [4].
[c]Reference [10].
[d]Reference [11].

transverse magnetic field [21]. The comparison of different hydrogen optical frequencies (for example, 1S-3S and 2S-8S/D) will reduce the uncertainty in the Lamb shift to a few parts in 10^6 and that in the Rydberg constant to a few parts in 10^{12}.

The authors are indebted to B. Cagnac for many stimulating discussions. They thank C. D. Thompson for assistance with this experiment and P. Indelicato for the communication of preliminary results for the calculation of the Lamb shifts of the excited levels. They thank also M. I. Eides, E. A. Hinds, K. Pachucki, and P. Mohr for communicating their results before publication. This work is partially supported by the Bureau National de Métrologie, by the Direction des Recherches et Etudes Techniques and by the European Community (SCIENCE cooperation Contract No. SC1*-CT92-0816 and network Contract No. CHRX-CT93-0105).

[1] See, for example, J.R. Sapirstein and D.R. Yennie, in *Quantum Electrodynamics,* edited by T. Kinoshita (World Scientific, Singapore, 1990); K. Pachucki *et al.,* in "Electron Theory and Quantum Electrodynamics–100 Years Later" (Plenum, New York, to be published); P. Mohr, in "Atomic, Molecular and Optical Physics Reference Book," edited by G.W.F. Drake (American Institute of Physics, New York, to be published).
[2] L.N. Hand, D.G. Miller, and R. Wilson, Rev. Mod. Phys. **35**, 335 (1963).
[3] G.G. Simon, C. Schmitt, F. Borkowski, and V.H. Walther, Nucl. Phys. **A333**, 381 (1980).
[4] F. Nez *et al.,* Europhys. Lett. **24**, 635 (1993).
[5] T. Andreae *et al.,* Phys. Rev. Lett. **69**, 1923 (1992).
[6] W.E. Lamb and R.C. Retherford, Phys. Rev. **72**, 241 (1947).
[7] S.R. Lundeen and F.M. Pipkin, Phys. Rev. Lett. **46**, 232 (1981).
[8] E.W. Hagley and F.M. Pipkin, Phys. Rev. Lett. **72**, 1172 (1994).
[9] M.G. Boshier *et al.,* Phys. Rev. A **40**, 6169 (1989).
[10] M. Weitz *et al.,* Phys. Rev. Lett. **72**, 328 (1994).
[11] D.J. Berkeland, E.A. Hinds, and M.G. Boshier, Phys. Rev. Lett. **75**, 2470 (1995).
[12] S. Bourzeix, M.D. Plimmer, F. Nez, L. Julien, and F. Biraben, Opt. Commun. **99**, 89 (1993).
[13] J.C. Garreau, M. Allegrini, L. Julien, and F. Biraben, J. Phys. **51**, 2263 (1990); **51**, 2275 (1990); **51**, 2293 (1990).
[14] F. Nez *et al.,* Phys. Rev. Lett. **69**, 2326 (1992).
[15] F. Biraben, J.C. Garreau, L. Julien, and M. Allegrini, Rev. Sci. Instrum. **61**, 1468 (1990).
[16] K. Pachucki, Phys. Rev. Lett. **72**, 3154 (1994).
[17] R.N. Fell, I.B. Khriplovich, A.I. Milstein, and A.S. Yelkhovsky, Phys. Lett. A **181**, 172 (1993); K. Pachucki and H. Grotch, Phys. Rev. A **51**, 1854 (1995).
[18] M. Weitz, F. Schmidt-Kaler, and T.W. Hänsch, Phys. Rev. Lett. **68**, 1120 (1992).
[19] S.G. Karshenboim, JETP **79**, 230 (1994); M.I. Eides and V.A. Shelyuto, Phys. Rev. A **52**, 954 (1995).
[20] V.G. Pal'chikov, Yu.L. Sokolov, and V.P. Yakovlev, Metrologia **21**, 99 (1985).
[21] F. Biraben, L. Julien, J. Plon, and F. Nez, Europhys. Lett. **15**, 831 (1991).